Investigation of Polypyrrole and Polypyrrole-polyethyleneimine as Adsorbents for Methyl Orange Dye Adsorption

NORHABIBAH MOHAMAD*[1], NOORDINI M. SALLEH[1,2] AND HABIBUN NABI MUHAMMAD EKRAMUL MAHMUD[1]

[1]*Department of Chemistry, Faculty of Science, Universiti Malaya, Kuala Lumpur, Malaysia.*

[2]*Centre for Fundamental and Frontier Sciences in Nanostructure Self-Assembly, Department of Chemistry, Universiti Malaya, Kuala Lumpur, Malaysia.*

ABSTRACT

The present study has explored the adsorption properties of polypyrrole-based adsorbents (polypyrrole and polypyrrole-polyethyleneimine composite) as novel conducting polymers in adsorbing methyl orange (MO) (an anionic dye) effectively from aqueous solution. The adsorption characteristics of the prepared polymer-based adsorbents were characterized by BET, FTIR, FESEM, and XRD methods. The effectiveness of PPy-based adsorbents for MO dye adsorption was examined using the batch adsorption method. Different parameters were changed during the adsorption process, including contact time, solution pH, and adsorbent dosage. The highest BET surface area of the PPy-PEI composite was found to be 11.85 m^2/g, which is much greater than that of the pristine PPy having 8.54 m^2/g. The dye removal performance was obtained to be 79.1 % and 98.8 %, by pristine PPy adsorbent and PPy-PEI adsorbent, respectively, at the optimum condition of pH 3, adsorbent dosage of 0.1 g with a contact time of 120 minutes. The Langmuir isotherm model explained the adsorption data better than the Freundlich isotherm model, and the pseudo-second-order model adequately explained the kinetic data for both the adsorbents. The regeneration investigation demonstrated the effectiveness of reusing PPy-PEI composite adsorbents for up to three successive adsorption-desorption cycles. The prepared PPy-PEI composite adsorbents appeared to be very much effective in removing anionic dyes from aqueous solutions.

KEYWORDS: *Conducting Polymer, Polymer Composite, Adsorption, Methyl Orange, Polymerization.*

J. Polym. Mater. Vol. **40,** No. 3-4, 2023, 165-189

*Correspondence author e-mail: ekramul@um.edu.my, nhabibahmohd11@gmail.com
DOI : https://doi.org/10.32381/JPM.2023.40.3-4.4

1. INTRODUCTION

Dyes released from the effluents of numerous industrial sources such as textile, printing, leather, petroleum, plastic, and pharmaceutical sectors are known to be a major concern for environmental pollution worldwide due to its toxic effects [1]. A variety of treatment techniques, such as ion-exchange, chemical precipitation, oxidation, osmosis, and adsorption have been developed to remove dyes from wastewater or aqueous solutions [2]. However, the majority of these methods have significant drawbacks, such as insufficient material removal, expensive monitoring systems, high reagent and energy requirements, or the production of toxic waste that needs to be properly disposed [3]. Adsorption is currently regarded as one of the most promising approaches among the several strategies reported for the treatment of dye-containing wastewater since it is simple, efficiency, and low cost[4]. Moreover, the adsorption method has better secondary levels whereby it has the capability of reusing its adsorbent, ease of regeneration and low-cost operation [5]. From Table 1, It is clear that each method for removing colours from wastewater has its own benefits and drawbacks to consider[6]. Adsorption has gradually grown in favor of a technique for treating wastewater effluents,

Table 1: Advantages and drawbacks of commonly used methods for removal of pollutants from wastewaters

Methods	**Advantages**	**Disadvantages**
Ozonation	Applied in gaseous state no alternative of volume	Short half-life of ozone (20 mins)
Oxidative process (H_2O_2)	Simplicity of application	(H_2O_2) should be first activated
Fenton reagents	Effective decolourization of both soluble and insoluble dyes	Big sludge production
Photocatalysis	No sludge production	Formation of by products
Adsorption	Low cost, high efficiency for removal of different types of dyes and metal ions	Some adsorbents have low surface area, possible side reactions loss of adsorbents, performance dependents on wastewater characteristics
Ionic exchange	Regeneration, no adsorbent loss	Not effective all types of dyes
Electrochemical treatment	Degraded compounds are non-hazardous	High cost
Irradiation	Effective oxidation at lab scale	High cost, requires a lot of dissolved O_2
Biological process	Environmentally friendly, public acceptance, economically attractive	Slow process, needs adequate nutrients, narrow operating temperature range
Coagulation and precipitation	Effective for all dyes	High sludge production, high cost

including heavy metal ions and other forms of effluents besides dyes [4].

Apart from traditional polymeric adsorbents, conducting polymer-based adsorbents such as polypyrrole (PPy), polyaniline, polyacetylene, and polythiphene have drawn a lot of attention due to their potential applications in adsorbing different colours in aqueous solutions. However, compared to other conducting polymers, polypyrrole is more economical, easy to synthesise and environmentally friendly[7]. Polypyrrole can also be coupled with various surface-active compounds to make composite materials with increased dye ion sorption capacities. To remove different dyes from an aqueous environment, materials like sawdust, natural and synthetic zeolite, cellulose, activated carbon, chitin, or graphene are frequently used in conducting polymers such as polypyrrole[8].

Polypyrrole nanofibers has been reported to remove MO dye, a typical anionic azo dye from aqueous solution with excellent adsorption capacity of 169.55 mg/g with the optimum condition at 120 min equilibrium time, 150 mg/L of MO initial concentration, temperature 298 K, and pH range from 7-10[9] (Xin *et al*., 2015). A study[10] reported the adsorption of MO dye from aqueous solution using ferroferric oxide/polypyrrole (Fe_3O_4/PPy) magnetic composite in the presence of ferric chloride hexahydrate, polyvinylpyrrolidone and γ-Aminopropyltriethoxysilane (KH-550) and achieved a maximum adsorption capacity of 149.48 mg/g for MO adsorption at 25°C with a contact time of 45 min[11]. Investigation on the adsorption of MO azo dye from aqueous solutions used polypyrrole-based graphene oxide that has undergone alkali activation (PACK). The equilibrium adsorption capacity, saturation rate, breakthrough point, and exhaustion periods for the column operations were determined to be 57.21 mg/g, 87%, 90, and 290 min, respectively. PANI/PPy polymer composite nano-fibers made by oxidative chemical polymerization were shown[12] to have good anionic dye adsorption properties. A study[13] reported that a novel adsorbent of PPy@magnetic chitosan nanocomposite was synthesized for the removal of MO and Cr (VI) from aqueous solution. The authors reported maximal removal capacities of MO and Cr (VI) over this magnetic polymer nanocomposite reached 95 and 105 mg/g, respectively after 40 minutes of contact time at the pH value between 2 and 4.5.

Polyethyleneimine (PEI) and glutaraldehyde crosslinking was successfully modified by persimmon tannin (PT) to a cationic state to create a green and effective bioadsorbent (PTP) for methyl orange (MO) dye [14]. It was reported that the maximum adsorption capacity of 225.74 mg/g was achieved for MO dye at 323 K and a pH of 4 when the initial concentration of MO was 35 mg/L, the PTP bioadsorbent dosage was 15 mg, and an equilibrium time of 120 min was employed. On the other hand, the adsorption performance of spent tea leaves (STL) modified with polyethylenimine (PEI) on an anionic dye, namely Reactive Black 5 (RB5) and MO, was investigated from simulated wastewater and it showed that although the modification of STL surface with PEI reduced the STL surface area but the adsorption efficiency of PEI-STL rose as contact time increased, and the maximum removal percentage of 84.1% was achieved at ~120 min with adsorption capacity of 21.0 mg/g [14].

Various natural and synthetic adsorbents for MO have been studied for its removal from effluents. However, it is still showing that the adsorption capacities of these adsorbents for removing dyes from wastewater are not high. Therefore, the creation of a novel, highly effective adsorbent is essential for the elimination of MO from wastewater. This research study is to explore the potentiality of polypyrrole-polyethyleneimine (PPy-PEI) as an adsorbent for anionic MO dye from wastewater since no effort has been made to evaluate the adsorption properties of this material towards MO dyes from wastewater.

In this current study, the adsorption performance of polypyrrole-polyethyleneimine has been evaluated to adsorb methyl orange dye from aqueous solution in order to realize the synergistic effect of both polypyrrole and polyethyleneimine as adsorbents. This new adsorbent has been prepared by chemical oxidative polymerization of pyrrole with the combination of polyethyleneimine at different conditions. The effects of different parameters such as contact time, adsorbent doses, and solution pH have been investigated in this adsorption study as well as the regeneration of the adsorbent.

2. EXPERIMENTAL

2.1. Materials

All chemicals used were of analytical reagents grades. The monomer, pyrrole was purchased from Sigma-Aldrich, MO dye was purchased from R&M Chemicals and polyethyleneimine (PEI) from Sigma-Aldrich. The oxidant, anhydrous ferric chloride ($FeCl_3$) was purchased from Sigma-Aldrich. The pH of the working solution was controlled by the application of HCl and NaOH (Merck). All solutions were prepared with deionized water. All these chemicals are mentioned in Figure 1.

2.2 Synthesis of Polypyrrole

Initially, different pyrrole monomer to oxidant ratios were used to produce polypyrrole (1:0.5, 1:1, 1:2 and 1:3). In a nutshell, 1.342 g of pyrrole monomer was dissolved in 20 mL of deionized water, and 5.406 g of anhydrous $FeCl_3$ oxidant was dissolved in an additional 80 mL of deionized water (1:1 mole ratio of monomer to oxidant). The $FeCl_3$ oxidant solution was then added to the pyrrole solution, agitated for three hours at room temperature at 150 rpm, to produce PPy polymer. The initial light green tint turning black indicated the formation of polypyrrole. The polypyrrole solution was filtered and repeatedly rinsed with deionized water to remove excess reactants producing a colourless filtrate. The recovered polymer product was subsequently dried for 24 hours at 65°C.

2.3 Synthesis of PPy-PEI Nanocomposite

Various mole ratios of monomer to oxidant (1:0.5, 1:1, 1:2 and 1:3) were studied. Following the same steps as the synthesis of PPy solution, 1.342 g of pyrrole monomer was first dissolved in deionized water, followed by the oxidant solution and 1.0 g of polyethyleneimine. The mixture was diluted with deionized water to make 100 mL before being added to the pyrrole solution to begin the polymerization of the pyrrole. The transition of the precipitate's colour from light green to black suggested the creation of a PPy-PEI polymer composite. With deionized water, the mixture was rinsed numerous times. The product was then dried in the chemical oven for 24 hours at 65°C.

2.4 Adsorption Experiments

All adsorption experiments were conducted for known concentration of methyl orange dye with the prepared pristine PPy and PPy-PEI composites. Typically, a 50 ml solution of known dye concentration were mixed in respective beakers with different adsorbent dosages (0.05 g to 0.4 g) of pristine PPy and PPy-PEI composite, and different ranges of (1 to 13). The mixture was shaked in a shaking incubator at 150 rpm for various contact times (30 min to 300 min). The adsorption

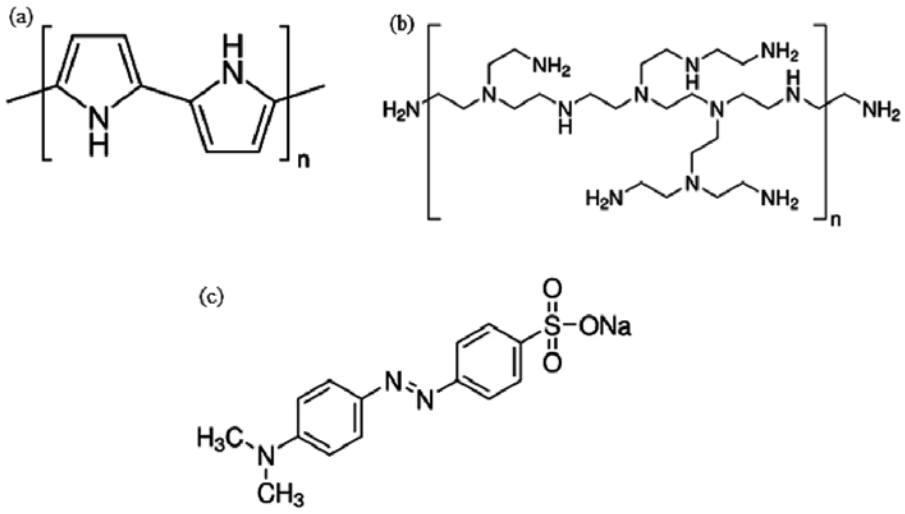

Fig. 1. Molecular structure of (a) PPy (b) PEI and (c) MO dye.

isotherm models of Freundlich and Langmuir were investigated. A kinetic investigation was also conducted.

2.5 Ultra-violet Spectrophotometer Analysis

Filtration was the final step to remove the adsorbent from the treated solution. A UV analysis was performed on the solution's filtrate. with a wavelength of 464 nm for MO dye, as shown in Table 2. The dye removal efficiency was calculated by the following equation:

$$\% \, Efficiency = \frac{Ci - Cf}{Ci} \times 100\%$$

Where, C_i (mg/L) and C_f (mg/L) are the concentrations of dyes at the initial and final (before and after adsorption), respectively.

2.6 Regeneration

Acidic and alkaline solutions were used to desorb MO dye from the surface of PPy-based adsorbents in order to examine the regeneration ability. Usually, the powders from the used PPy-based adsorbents were placed in the flasks. During the regeneration procedure, 50 mL of deionized water, 50 mL of 0.1 M HCl, or 50 mL of 0.1 M NaOH solution were applied individually. The regenerating adsorbent was then utilised in additional adsorption tests. The UV-vis spectrophotometer was then used to calculate the adsorption and desorption of dye.

2.7 Characterization

The surface analyzer used N_2 adsorption at 77.4 K to calculate the Brunner-Emmett-Teller (BET)'s surface area. Following the t-method, the pore structure of this adsorbent was identified. FESEM was used to examine the surface morphology of the PPy-PEI polymer-based adsorbents both before and after adsorption. Compared to SEM, FESEM produces images with higher resolution thanks to its high-powered, concentrated, and monochromatic electron beam that enters the sample. Field emissions were used to source and emit electrons that were accelerated at extremely high speeds and high voltages between 0.5 and 30 kV. FTIR was conducted using Attenuated Total Reflectance (ATR) method. Prior to and following dye adsorption, conducting polymer's functional groups were identified using FTIR. Each sample underwent 16 scans in the frequency range of 4000-550 cm^{-1} at a resolution of 4 cm^{-1}. The X-ray diffraction (XRD) patterns were recorded on a powder sample for phase recognition of crystalline materials. The XRD patterns were recorded in the 2θ range of 5-90° with step time 1.25 sec using Cu Kα radiation (λ=1.5406).

TABLE 2: The physical properties of the investigated dye

Name	Methyl orange (MO)
Molecular formula	$C_{14}H_{14}N_3SO_3Na$
Molar mass (g/mol)	327.33
λ_{max} (nm)	464

3. RESULTS AND DISCUSSION

Figure 2 shows that the adsorption efficiency of pristine PPy and PPy-PEI composite adsorbent at pH 3 using 0.1 g of adsorbent with a contact time of 120 min for the removal of methyl orange (MO) dye from aqueous solution. The adsorbents were prepared by different monomer to oxidant ratios (1:0.5, 1:1, 1:2, and 1:3), respectively. It was observed that the adsorption efficiency of pristine PPy adsorbent prepared from using 1:1 mole ratio of monomer to oxidant, exhibited the maximum adsorption efficiency of 78.5 %, whereas, the maximum adsorption efficiency shown by the PPy-PEI adsorbent prepared from using 1:1 mole ratio of monomer to oxidant, exhibited much higher adsorption of 98.6 %. The increased in adsorption efficiency by PPy-PEI composite adsorbent shows that this composite adsorbent is more effective to treat wastewater to remove MO dye than the pristine polypyrrole adsorbent. Here, apart from polypyrrole, the amine group coming from polyethyleneimine appears to be the added site of dye adsorption in polypyrrole-polyethyleneimine (PPy-PEI) structure resulting in higher adsorption. Thus, the synergetic effect of both polypyrrole and polyethyleneimine for adsorption has been realized in PPy-PEI adsorbent. It was observed that the higher surface area of PPY-PEI played a vital role in adsorption than the pristine polypyrrole having a lower surface area.

It can be mentioned here that the polymer produced from higher mole ratio of monomer to oxidant, exhibited lower adsorption efficiency due to the formation of densely formed structure of polypyrrole which restricted the adsorption of dyes. However, as the amount of oxidant increased (1:2 and 1:3), it resulted in a decreased percentage of dye removal due to hard and compact polymer formation which buried the available active sites for adsorption. Therefore, fewer free active sites were available for the adsorption to take place. The low monomer to oxidant ratio (1:0.5) resulted in a low adsorption efficiency due to incomplete polymerization process producing a very thin, soft coating of powder that appears to be very difficult to manage [15]. Hence, the ideal removal of MO dye was at the mole ratio of 1:1 of pyrrole monomer to oxidant for both types of PPy-based adsorbents. Consequently, the mole ratio of 1:1 of pyrrole to oxidant was used for all the experiments.

3.1 BET Analysis

One of the variables for assessing the adsorption performance of the adsorbent is its surface area, pore size, and volume distribution. The produced PPy-based adsorbents' comparative BET surface area, pore volume,

and pore size characteristics are presented in Table 3. It was discovered that as oxidant molar concentration increased, both the BET surface area and pore volume decreased. For pristine PPy adsorbent prepared from using 1:0.5 mole ratio of monomer to oxidant produced the higher surface area in the BET surface measurement. However, pristine PPy adsorbent prepared from using 1:1 mole ratio of monomer to oxidant demonstrated better adsorption efficiency comparing with the adsorption performance among all the polymers produced from using various mole ratios. The polymer produced from using a lower monomer to oxidant ratio (1:0.5) appeared very thin and soft powder that was very difficult to handle and therefore, it was not considered to use for adsorption. However, the results also revealed that the PPy-PEI composite adsorbents had higher values for

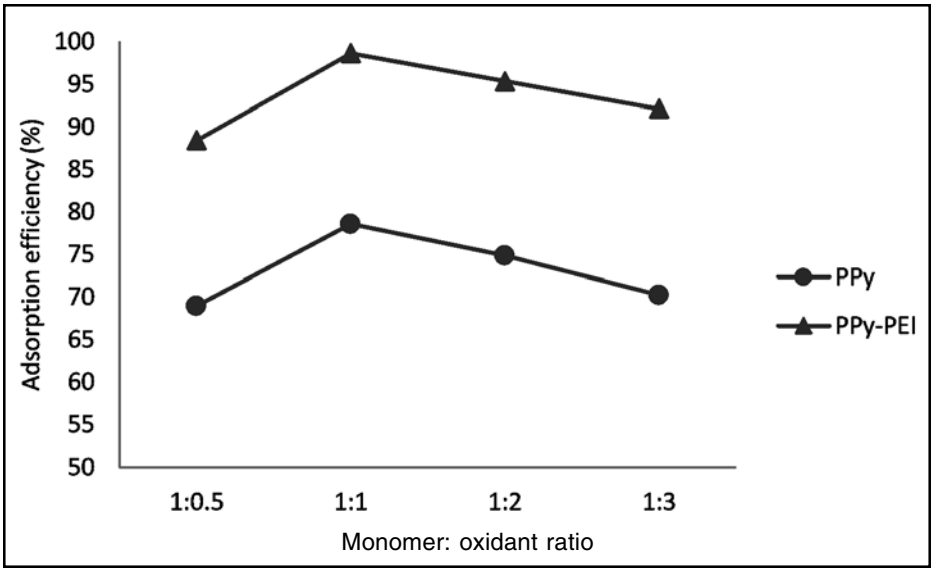

Fig. 2. Adsorption efficiency on the adsorption of 100 ppm methyl orange dye by pristine PPy and PPy-PEI composite adsorbent.

pore volume distribution and BET surface area compared to pure PPy adsorbents. The maximum BET surface area of the PPy-PEI composite produced from using 1:1 mole ratio of monomer to oxidant was found to be 11.85 m^2/g, which is significantly higher than the surface area produced by pristine PPy (1:1), that is, 8.54 m^2/g. Adding PEI to PPy significantly increased the adsorbent's surface area. The increase could be attributed to the successful adsorption of polypyrrole throughout the polyethylenimine pore matrix. In comparison to pristine PPy adsorbent, the PPy-PEI composite adsorbent has a better adsorption potential due to more binding sites emerged from higher surface area of PPy-PEI composite adsorbent. Similar findings have been reported by other authors [16].

3.2 FESEM Analysis

The morphology of the pristine PPy and PPy-PEI polymer composite were studied using field emission scanning electron microscopy. The FESEM micrographs of as-prepared pristine PPy before and after adsorption are shown in Figures 3 and Figure 4, respectively. From Figure 3 (a), the FESEM images of pristine PPy exhibited uniform spheres with abundance pores of smooth cloud structure and the cauliflower-like compact surface of typical polypyrrole revealed the successful synthesis of polypyrrole. The surfaces of the material showed the presence of several spherical particles of about internal diameter of 195-345 nm, with a higher magnification of x 130,000 as shown in Figure 3 (b). From Figure 3 (c), there was little observable of FESEM images after dye adsorption on pristine PPy. The FESEM images show several irregularities of the polymer's morphology and thus, it indicates the dye adsorbate has successfully been adsorbed on the surface of adsorbent. Figure 3 (d) clearly shows that the surface of the adsorbed sample becomes denser with an

TABLE 3: Characteristics of Polypyrrole and Composite, Surface area Measurements and Pore Volume Distribution

Adsorbent	Pyyrole: oxidant	BET surface area (m^2/g)	Total pore volume (cm^3/g)	Pore size (Å)
PPy	1:0.5	9.25	0.02603	82.26
PPy	1:1	8.54	0.02283	85.74
PPy	1:2	7.69	0.01257	87.47
PPy	1:3	6.70	0.01205	87.76
PPy-PEI	1:1	11.85	0.02940	52.76

average internal diameter of 172-223 nm, which demonstrates the successful dye adsorption by PPy. Several other studies also reported the similar scanning images of typical PPy [10,11,16,17].

The FESEM micrographs of PPy-PEI polymer composite before and after adsorption are shown in Figure 4. Figure 4 (a), shows a smooth cloud like structure of PPy-PEI composite but rougher than pristine PPy with a simple π-π bonding structure. The incorporation of PEI into PPy shows a porous morphology. The structure formed exhibited like honeycomb or the circular holes that are evenly distributed on the surface. As seen in Figure 4 (b), the PPy-PEI composite owned homogeneous morphology with an average diameter of 400-550 nm before dye adsorption. After dye adsorption, the solid PPy-PEI composite exhibited a rough surface, [Figure 4 (c)] which proved helpful for removing dye from an aqueous solution [9] with increased dye adsorption capacity [4]. The FESEM images also reveal a distinctive structure made up of globules of PPy-based adsorbents While in Figure 4 (d), the FESEM image shows clearly that the surface of the adsorbed sample becomes denser as it was observed for

polypyrrole but with an average diameter of 160-190 nm which could be referred to dye adsorption. The presence of both adsorbent-adsorbate simply increases the density of surface topography and have lesser distance

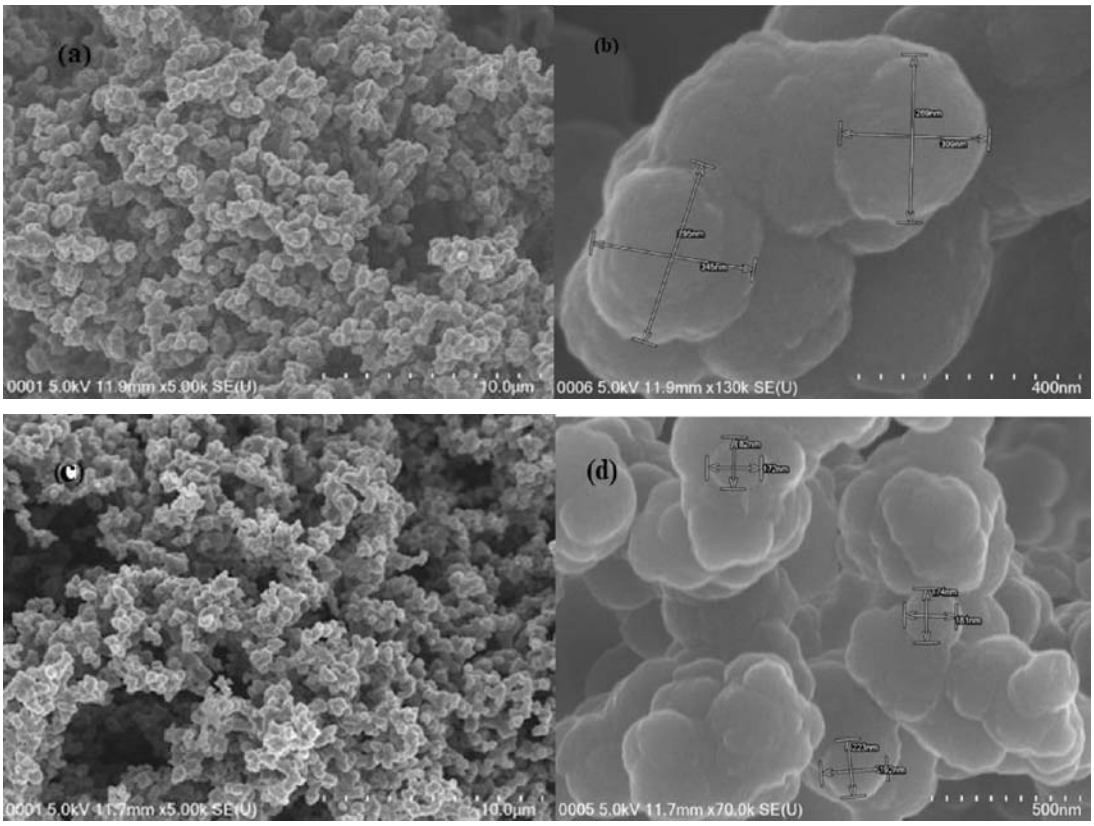

Fig. 3. FESEM image of pristine PPy with different magnifications (a) before adsorption × 5.00 k; (b) before adsorption × 130.0 k; (c) after adsorption × 5.00 k; (d) after adsorption × 70.0 k

of particles. Additionally, a greater amino group on the PEI polymer chain stabilizes the particles with strong static repulsion and steric hindrance, which is the cause of the reduction in particle sizes [4].

3.3 FTIR Studies

Figure 5 displays the ATR-FTIR spectrum of the as-prepared PPy adsorbent both before and after dye adsorption. All of the band locations of the PPy adsorbent before adsorption were noticeably changed to various wavenumbers after the dye adsorption, which caused some noticeable changes in the spectra. Before MO dye adsorption, observable bands were at 3744 cm^{-1}, 2081 cm^{-1}, 1635 cm^{-1}, 1519 cm^{-1}, 1436 cm^{-1}, 1275 cm^{-1}, 1129 cm^{-1}, 998 cm^{-1}, 832 cm^{-1}, 751 cm^{-1},

646 cm^{-1}, and 572 cm^{-1}. However, after adsorption of MO dye, it was found that the bands have been shifted to 3749 cm^{-1}, 2066 cm^{-1}, 1697 cm^{-1}, 1540 cm^{-1}, 1462 cm^{-1}, 1291 cm^{-1}, 1156 cm^{-1}, 1038 cm^{-1}, 884 cm^{-1}, 779 cm^{-1}, 662 cm^{-1}, and 600 cm^{-1}, respectively, indicating that MO dye was successfully adsorbed onto the adsorbent surface. The main distinctive peaks that typically confirmed the synthesis of polypyrrole were those identified at 1635 cm^{-1} to 1436 cm^{-1} due to stretching vibrations of C=C of pyrrole ring, the C-N stretching at 1275 cm^{-1}, and the C-H in-plane deformation at 1129 cm^{-1}. In addition, it was evident that the peak

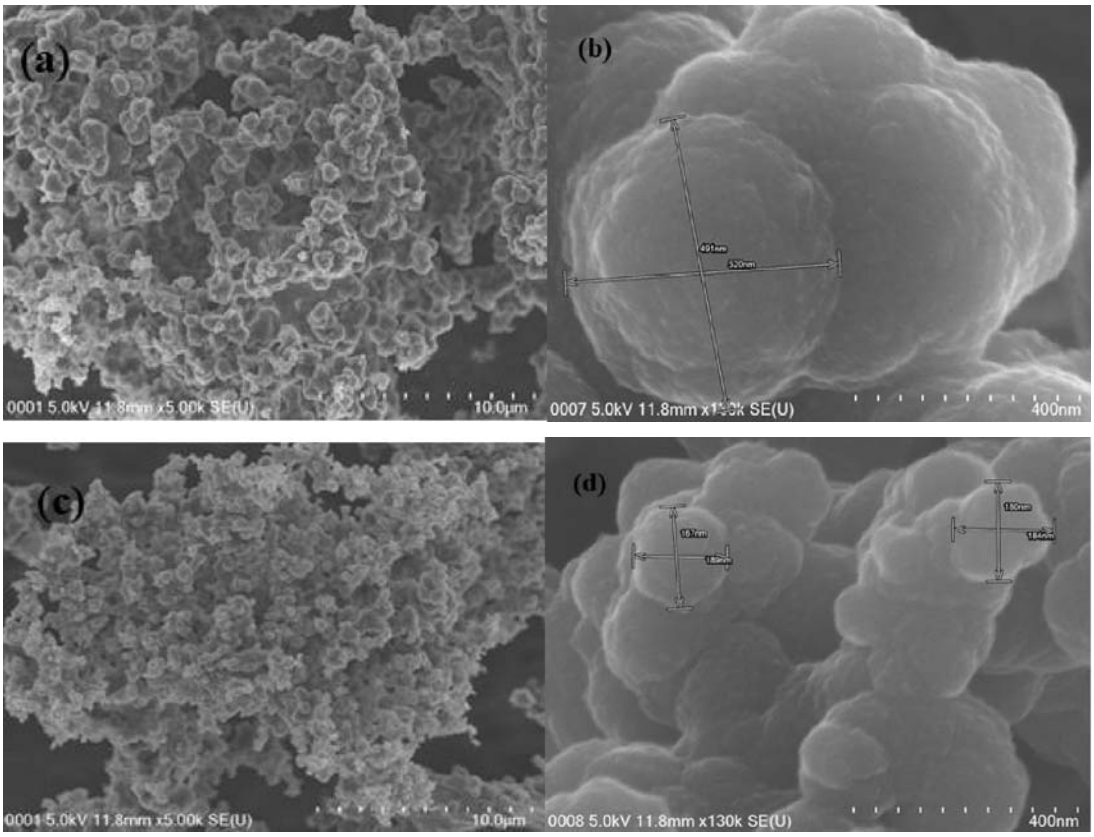

Fig. 4. FESEM image of PPy-PEI composite with different magnifications (a) before adsorption × 5.00 k; (b) before adsorption × 130.0 k; (c) after adsorption × 5.00 k; (d) after adsorption × 130.0 k

at 2081 cm^{-1}, which was attributed to the N-H stretching vibration due to the pyrrole ring, was observed at a lower wavenumber and slightly disappeared after adsorption, supporting the involvement of the relevant functional groups in the formation of strong chemical bonds during dye adsorption. After MO adsorption, the peak at 998 cm^{-1}, which is due to C-N stretching or

C-H bending prior to adsorption, has slightly shifted to a sharp peak at 1038 cm^{-1}. These modifications proved that MO molecules and PPy surface functional groups were involved. In Table 4, all band locations are listed. There was also good agreement with those reported in the literature on the characteristics of PPy spectrum [16-18].

It has been observed that some of the band locations of the PPy-PEI composite significantly shifted to other wavenumbers compared to PPy spectrum indicating the successful incorporation of PEI in PPy structure. Figure 6 shows the ATR-FTIR spectra of PPy-PEI composite before and after adsorption of MO dye. All the characteristic band positions of ATR-FTIR as can be seen in Table 5, support the adsorption of MO dye by PPy-PEI composite adsorbent. The bands at 3752 cm^{-1}, 1707 cm^{-1}, 1641 cm^{-1}, and 1537 cm^{-1} observed in PPy-PEI spectrum before adsorption of MO dye have shifted to lower wavenumbers of 3743 cm^{-1}, 1698 cm^{-1}, 1639 cm^{-1}, and 1534 cm^{-1}, respectively, while the bands at 3000 cm^{-1}, 1436 cm^{-1}, 1282 cm^{-1}, 1144 cm^{-1}, 1037 cm^{-1}, 877 cm^{-1}, 775 cm^{-1} and 658 cm^{-1} observed in PPy-PEI spectrum before adsorption of MO dye have shifted to higher wavenumbers of 3116 cm^{-1}, 1463 cm^{-1}, 1298 cm^{-1}, 1150 cm^{-1}, 1039 cm^{-1}, 887 cm^{-1}, 776 cm^{-1} and 664 cm^{-1}, respectively, after adsorption.

The distinctive high-intensity peak at 1537 cm^{-1} due to the pyrrole ring's asymmetric stretching vibrations of C=C has shifted to 1534 cm^{-1} after dye adsorption. The other adsorption features of the PPy-PEI polymer adsorbent revealed that the band at 1641 cm^{-1} due to the symmetric N-H bending shifted to 1639 cm^{-1} and the band at 1282 cm^{-1} due to C-N

TABLE 4: Chemical bonding for PPy adsorbent before and after adsorption of MO dye

Type of vibration	Peak position before adsorption (cm^{-1})	Peak position after adsorption (cm^{-1})
O-H stretching	3744	3749
N-H stretching	2081	2066
C=C stretching	1635	1697
C=C stretching	1519	1540
C=C stretching/C-N stretching	1436	1462
C-N stretching	1275	1291
C-H bending	1129	1156
C-H bending/ S=O stretching	998	1038
C-H bending	832	884
C-H bending	751	779
C-H bending	646	662
C-H bending	572	600

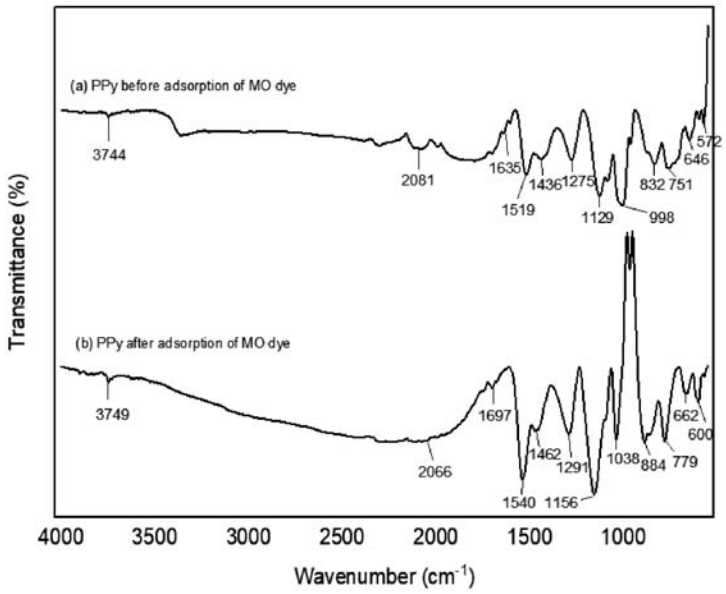

Figure 5. ATR-FTIR analysis for pristine PPy before and after MO dye adsorption.

stretching vibration shifted to 1298 cm^{-1} after the dye adsorption [4,19]. These modifications proved that MO molecules and PPy-PEI surface functional groups were involved. Similar results have been reported by other authors [14]. The FTIR results also support the formation of PPY-PEI composites. The differences in peak positions assigned to pristine PPy and PPy-PEI without adsorption in Tables 4 and 5, respectively, indicate the successful incorporation of PEI in PPy structure producing PPy-PEI composite with more adsorption active sites leading to a very efficient dye removal [3].

3.4 XRD Analysis

The crystalline nature of PPy-PEI composite was determined from XRD analysis. The XRD analysis of PPy-PEI polymer composite before and after MO adsorption were done and the X-ray diffraction patterns obtained are shown in Figure 7. Before MO adsorption, the main peak showed a broad peak at $2\theta = 26.2°$ which clearly indicates the amorphous nature of polypyrrole. In the case of PPy-PEI composites, after dye adsorption, the broad peak observed has been shifted backward around $2\theta = 15.5°$ and a new sharp peak has appeared at $2\theta = 25.1°$. The XRD analysis of PPy-PEI after adsorption showed little shift in 2θ values from 26.2° to 25.1°. According to this pattern, the evidences of polymer composite formation and MO dye adsorption can also be obtained. The X-ray diffraction patterns that have been observed are comparable to the diffraction patterns reported for polypyrrole and its composites by others [5,9,11,13].

3.5 Effect of Solution pH

The pH of the solution may have an impact on the adsorbent's surface charge, as well as the

TABLE 5: Chemical bonding for PPy-PEI adsorbent before and after adsorption of MO dye.

Type of vibration	Peak position before adsorption (cm^{-1})	Peak position after adsorption (cm^{-1})
O-H stretching	3752	3743
N-H stretching	3000	3116
C=C stretching	1707	1698
N-H bending	1641	1639
C-C=C asymmetric stretch	1537	1534
C-H bending	1436	1463
C-N stretching	1282	1298
C-H in plane deformation	1144	1150
S=O stretching	1037	1039
C-H bending	877	887
C-H bending	775	776
C-H bending	658	664
C=C bending	-	595

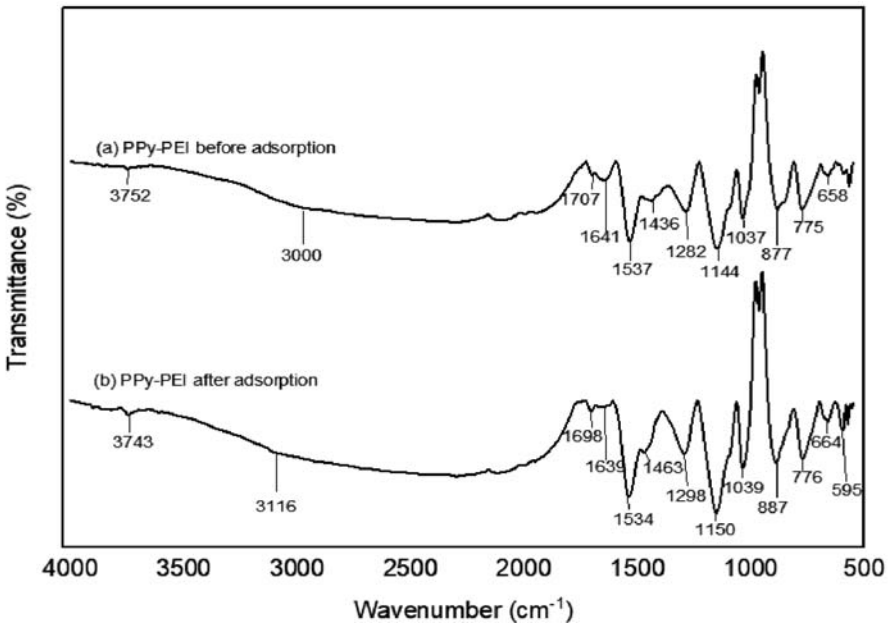

Fig. 6. ATR-FTIR analysis for PPy-PEI composite before and after MO dye adsorption.

structure of the dye. With an initial concentration of 100 ppm dye, the impact of pH in the solutions on the adsorption effectiveness of MO was therefore investigated at various pH values ranging from 1 to 13. 0.1 mol L^{-1} HCl or 0.1 mol L^{-1} NaOH solutions were added to modify the pH values. Accordingly, 0.1 g of each PPy adsorbent was treated with 50 mL of MO solution for a contact time of 120 minutes. From Figure 8, it was found that at pH 3 with a specific dosage and contact period, the maximum adsorption of 100 ppm of MO dye by pristine PPy adsorbent was 78 % while PPy-PEI composite adsorbent exhibited an adsorption of 97.8%. The adsorption effectiveness was shown to have the highest adsorption at pH 3, afterwards, the effectiveness of adsorption was found to reduce with pH increase. Therefore, this pH value of 3 was used for all the experiments.

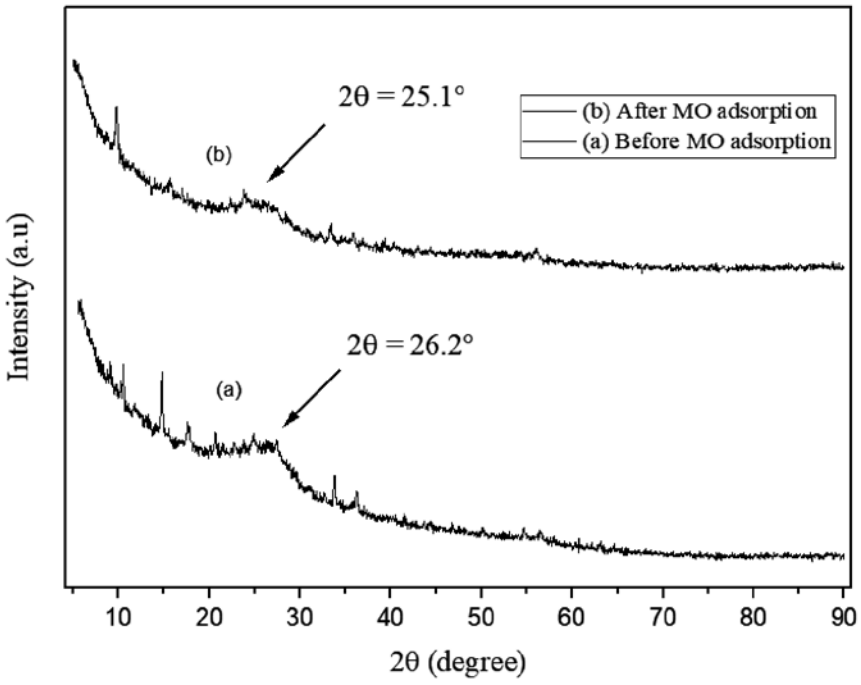

Fig. 7. XRD diffractograms for PPy-PEI before and after MO dye adsorption.

From the obtained results, it was observed that at a particular pH, PPy-PEI composite adsorbent exhibited higher adsorption performance compared to pristine PPy adsorbent due to the presence of PEI having more nitrogen containing groups in the compounds with polypyrrole structure. The effect of pH has impact on the surface charge on the pristine PPy adsorbent and PPy-PEI composite adsorbent. For the adsorption of dye

ions, the functional group -NH_2 in PPy and PEI is regarded as an active site. These -NH_2 group may undergo protonation to NH_3^+ depending on the pH of the solution, and the degree of protonation will depend on the pH of the solution. In general, at a low pH, the adsorption efficiency increases for anionic MO dye adsorption. This happens due to the increase of positive charges on the solution interface together with the positive charges on the adsorbent surface, which results in an increase of positive charges for anionic MO dye adsorption. At a higher solution pH, adsorption efficiency decreases for anionic MO dye adsorption [20].

3.6 Effect of Adsorbent Dosage

To essentially minimize the doses of PPy-based adsorbents needed for the adsorption process, the effect of adsorbent dosage on MO dye removal was examined. Different PPy-based adsorbent masses, ranging from 0.05 to 0.4 g, were used for the adsorption with optimum conditions for MO dye at a solution pH of 3 and 120 min contact time. As shown in Figure 9, the maximum adsorption efficiency was exhibited at 79.1 % by pristine PPy adsorbent and 98.3 % by PPy-PEI composite adsorbent, both by 0.1 g of the prepared adsorbent.

From the obtained results, it was observed that PPy-PEI composite adsorbent exhibited higher adsorption performance in a range of adsorbent dosage compared to pristine PPy adsorbent. By considering the adsorbent loading to a minimum during adsorption, all adsorption experiments were carried out using a PPy loading of 0.1 g for MO dye removal. Since the polymer adsorbent aggregates and decreases the adsorbents' active surface area or contact surface area, the larger adsorbent dosage may not be beneficial because the adsorbent's active sites are saturated. This lowers the adsorption

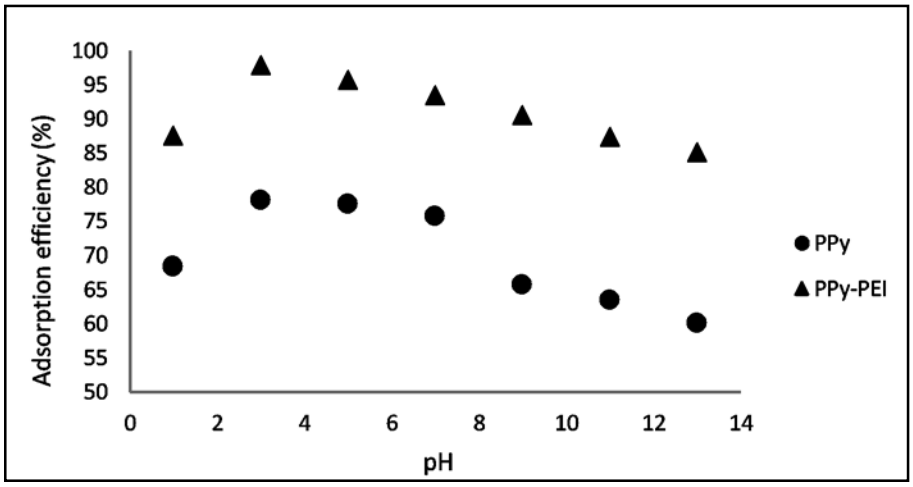

Fig. 8. Effect of solution pH by pristine PPy and PPy-PEI composite adsorbents on adsorption of 100 ppm MO; adsorbent dosage 0.1 g of adsorbent dose; contact time 120 min and 1:1 mole ratio of Py:$FeCl_3$.

effectiveness. The similar findings have been reported by other authors [14,16,21].

3.7 Effect of Contact Time

The effect of contact time on the adsorption of MO dye by PPy-based adsorbents was carried out at a contact time ranging from 30 to 300 min for 100 ppm initial dye concentration at pH 3 and 0.1 g adsorbent dose. Figure 10 depicts how the amount of time in contact with the pristine PPy adsorbent and the PPy-PEI composite adsorbent affects the removal of 100 ppm MO dye. The adsorption results on contact time show that the maximum adsorption efficiency of 79.0 % and 98.8% was obtained by pristine PPy and PPy-PEI composite, respectively, with a contact time of 120 min.

It was found that the adsorption of MO was found to increase initially till 20 min, and beyond that it became steady. This could be explained by the fact that there were many open surface areas accessible for adsorption to occur at in the beginning and that it happened

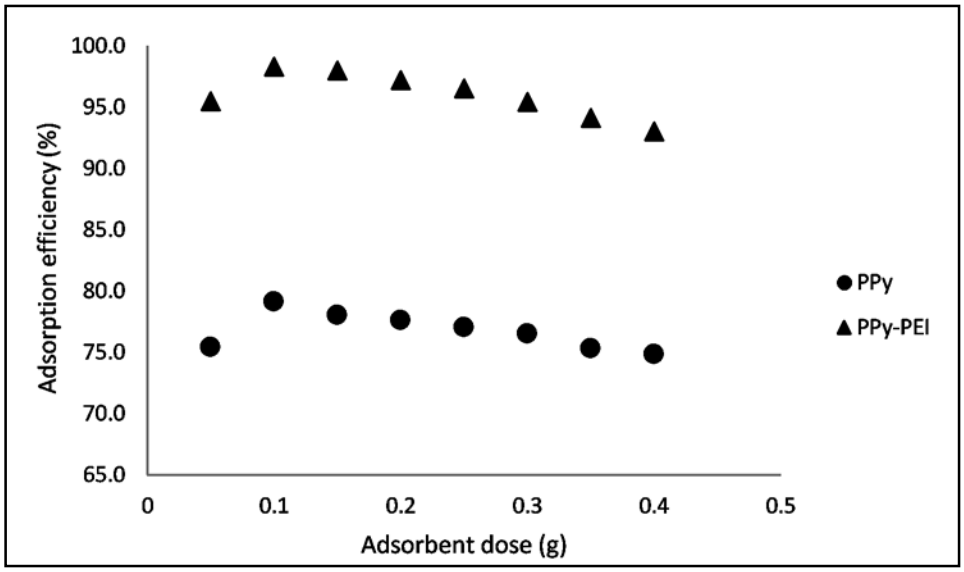

Fig. 9. Effect of adsorbent dosage by pristine PPy and PPy-PEI composite adsorbents on adsorption of 100 ppm MO; pH 3; contact time 120 min and 1:1 mole ratio of Py:$FeCl_3$.

quickly. Due to the repelling forces between the solute molecules on the solid and in the aqueous phases, the number of unoccupied surface sites decreased as the adsorption process continued and they were challenging to occupy [22]. As a result, the adsorption had now reached equilibrium. Other reporters have noted the same pattern [9,11,13,16,22-24].

3.8 Adsorption Kinetic Study

To comprehend the dynamics of the adsorption process in terms of the order of rate constant, the kinetics of adsorption data

was processed. Understanding the adsorption kinetic is crucial for creating future large-scale adsorption processes that are both feasible and efficient [25]. Pseudo-first-order and pseudo-second-order models were applied to the adsorption kinetic data in order to investigate the behaviour of adsorption process of dye onto PPy-PEI composite. Table 6 shows the adsorption kinetic data of MO dye. The pseudo-first-order model was used to compute the maximal adsorption capacity, Q_e (mg/g), the amount of adsorption at time t (min), Q_t (mg/g), and the Lagergren rate constant of adsorption, K_1 (min-1) [26]:

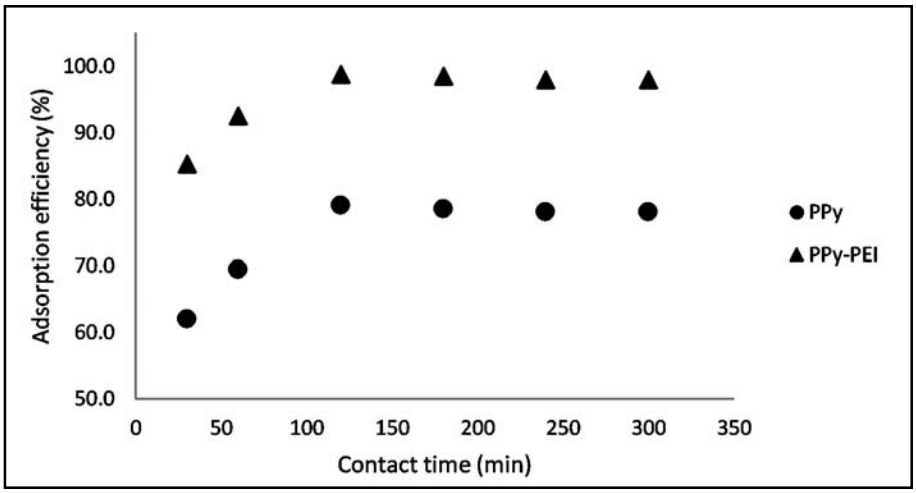

Fig. 10. Effect of contact time by pristine PPy and PPy-PEI composite adsorbents on adsorption of 100 ppm MO; pH 3; 0.1 adsorbent dose and 1:1 mole ratio of Py:$FeCl_3$.

$$\ln (Q_e - Q_t) = \ln Q_e - K_1 t$$

The intercepts and slope of the plot were used to compute the values of K_1 and Q_e of $\ln(Q_e - Q_t)$ versus t as shown in Figure 11 (a) and the correlation coefficients, R^2, and the predicted and experimental Q_e values are given in Table 6. The following is how the pseudo-second-order rate model is written [26]:

$$\frac{t}{Q_t} = \frac{1}{K\,Q_e^2} + \frac{t}{Q_e}$$

Where, K_2 is the pseudo-second-order rate constant of adsorption (g/mg min). K_2 and Q_e were determined from the intercepts and the slope of the plot of t/Q_t versus t, respectively, as shown in Figure 11 (b). As can be seen in Figure 11, the linearized form of the pseudo-second-order model had a strong correlation (R^2 = 0.9998 and 0.9997) when compared to the pseudo-first-order model (R^2 = 0.9340 and 0.9206). Hence, it demonstrates that the MO dye adsorption matches better with pseudo-second-order, indicating that chemisorption was the mechanism involved, whereby the adsorption process may also entail chemisorption, which involves sharing or transferring valence electrons between the surfaces of the adsorbent and adsorbate [19]. The pseudo-second-order kinetics model's

estimated Q_e values were also substantially closer to the experimental ones. Therefore, the rate processes could not be explained by the pseudo-first-order kinetics.

3.9 Adsorption Isotherms Study

An adsorption isotherm is a graph that represents the variation of the amount of adsorbate adsorbed on the surface of an adsorbent. In this research, two important isotherms, i.e., Langmuir isotherm and Freundlich isotherm models were selected. For each adsorbent, these models are used to balance the theoretical and experimental data. How the solute interacts with the adsorbent can be described using adsorption isotherms, and they are crucial in order to use adsorbent as efficiently as possible to remove dyes from aqueous solution [23]. One active site can only be occupied by one adsorbate molecule according to the Langmuir adsorption isotherm, which shows that a monolayer of adsorbate covers the surface of the homogeneous

TABLE 6. Adsorption kinetic model parameters for MO dye adsorption

C_0 (ppm)	Q_{exp}	Pseudo-first-order			Pseudo-second-order		
		Q_e	K_1	R^2	Q_e	K_2	R^2
100	49.40	17.9340	0.0111	0.9340	49.7512	0.007566	0.9998
300	94.80	5.7540	0.0175	0.9206	96.1538	0.002287	0.9997

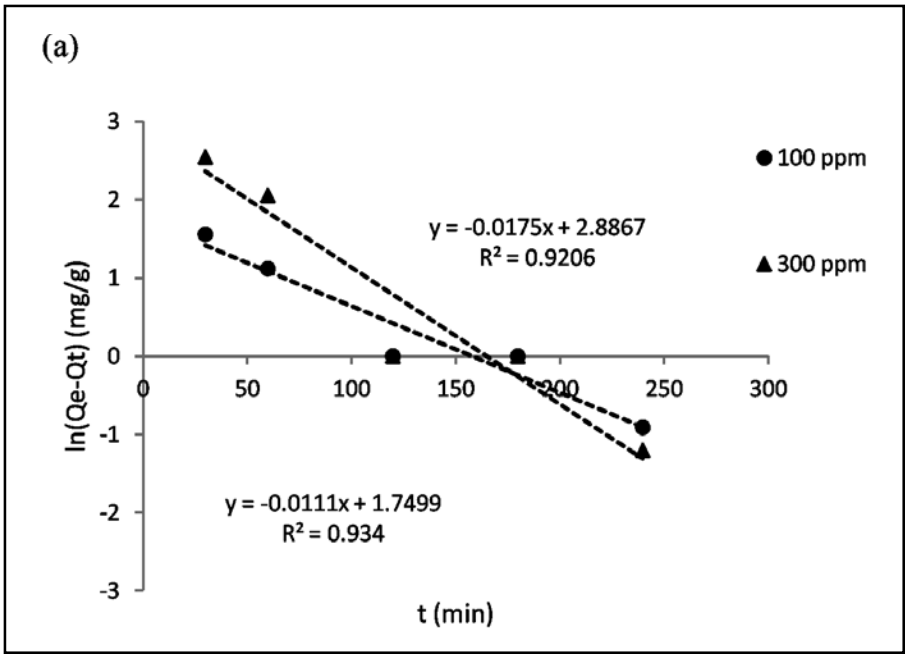

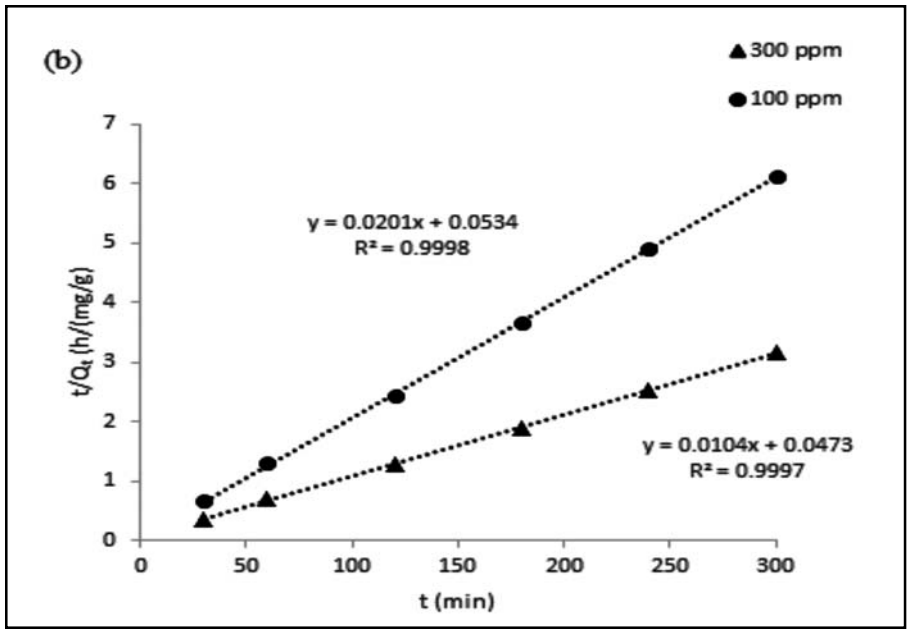

Fig. 11. Adsorption kinetic study of MO dye (a) Pseudo-first-order kinetic model (b) Pseudo-second-order kinetic model

adsorbent [27]. While the Freundlich model as an empirical equation, applied to non-ideal and multi-layer adsorption on the heterogenous surfaces [27]. The parameters for the Langmuir and Freundlich models of MO dye adsorption are all shown in Table 7 at temperatures of 27, 40 and 60, respectively. The Langmuir isotherm model equation is as follows [9]:

$$\frac{C_e}{Q_e} = \frac{C_e}{Q_m} + \frac{1}{Q_m b}$$

Where Q_m (mg/g) denotes maximum adsorption capacity, C_e (mg/L) indicates equilibrium MO dye concentration, Q_e (mg/g) indicates equilibrium adsorption capacity, and b (L/mg) denotes the Langmuir constant relating to the affinity of the adsorbent towards the adsorbate. The adsorption isotherm of MO at three different temperatures (27, 40 and 60°C are shown in Figure 12. A straight line was obtained when C_e/Q_e was plotted against C_e. The values of Q_m and b were calculated from the slopes and intercepts. The dimensionless separation factor, R_L, the key component of the Langmuir adsorption isotherm, is obtained as follows [9]:

$$R_L = \frac{1}{1+bC_0}$$

C_o represents the dye's original concentration. Adsorption favorability is shown by the separation factor, R_L value. According to [9], if this number is less than 1, it is favorable for adsorption ($0< R_L <1$) and if it is greater than 1, it is unfavourable ($R_L >1$) for adsorption. The equilibrium adsorption data matched to the Freundlich model, which assumes that the

solute would be adsorbed onto a heterogeneous surface, additional data was collected. The Freundlich model is stated as follows [9]:

$$\ln Q_e = \ln K_F + \frac{1}{n} \ln C_e$$

Where K_F and n are called Freundlich coefficients, and they represent the sorption capacity and the favorability of the adsorption process, respectively. The linearized Freundlich adsorption isotherm was estimated from the equation above. A straight line was obtained when was plotted against and, n and were calculated from the slopes and intercepts, respectively (Figure 12).

From the results obtained, it was observed that the correlation coefficients (R^2) shown by the Langmuir model are higher than the Freundlich model suggested that the adsorption sites onto the PPy-PEI adsorbent was homogeneous and it was a monolayer interaction between the composite surface and adsorbate. In addition to the homogeneity of the active sites, this was a sign of how the composite adsorption monolayer behaved. It also demonstrates the energetically comparable characteristics of the many active areas on the composite surface. The values of Q_m as found at various temperatures are also given in Table 7. The fact that Q_m decreased as temperature rose suggested that the exothermic nature of the process may be the reason why the removal of dyes was hindered by the rise in temperature [16]. In addition, the R_L values (in the range of 0–1) as shown in Table 7, demonstrates that the resulting adsorbent's adsorption process towards the examined adsorbates was successful. It should be noted that the very high adsorption capacity of MO on PPy-PEI adsorbent was mostly attributed to the synergistic effect of several absorption mechanisms [27].

In this context, it is worth mentioning that a number of different PPy composites or PEI composites as adsorbents have also been reported to follow Langmuir model for the adsorption of MO dye. Table 8 compares our findings to the values of the Langmuir parameters that have been reported for the adsorption of MO dye by various adsorbents. As demonstrated in Table 8, our values are within the range of the values that have been published. The findings show that the PPy-PEI composite adsorbent offers the potentiality to be an effective adsorbent for removing MO dye from wastewater.

3.10 Regeneration Study

A key factor in determining whether the adsorbent is economically viable is the

TABLE 7: Adsorption isotherm model parameters for MO dye adsorption

Temp. (°C)	Langmuir				Freundlich		
	Q_m	b	R_L	R^2	K_F	n	R^2
27 °C	232.56	0.0444	0.1838	0.9998	13.088	1.432	0.9894
40 °C	192.31	0.0763	0.1159	0.9994	17.875	1.616	0.9859
60 °C	169.49	0.1408	0.0663	0.9984	25.363	1.879	0.9788

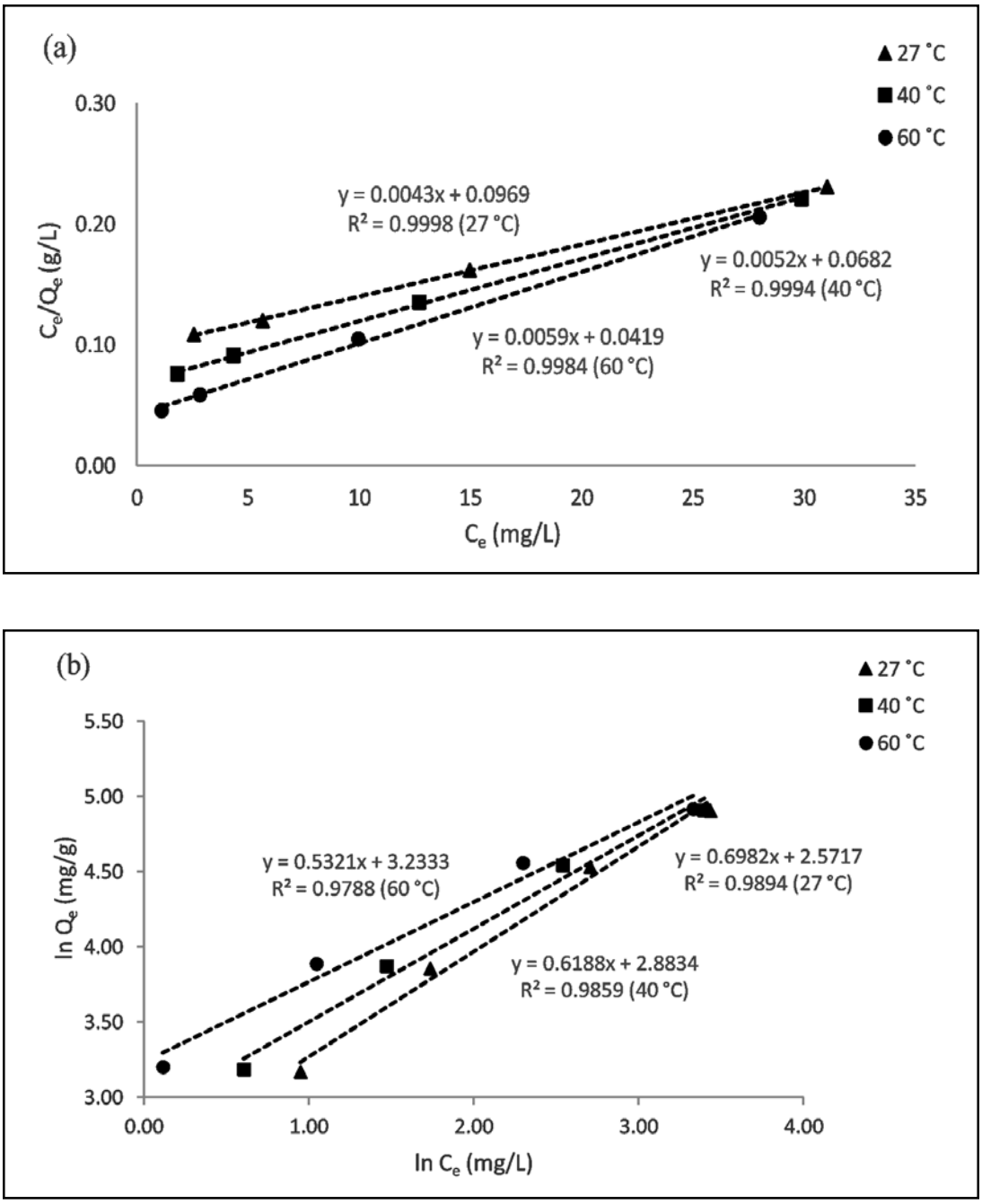

Fig. 12. Adsorption isotherm study of MO dye (a) Langmuir isotherm model (b) Freundlich isotherm model.

TABLE 8: Comparison of adsorption capacities of resulting adsorbent with previously reported adsorbents for MO uptake

Type of adsorbent	Dyes	Q_{max} (mg/g)	References
PEI modified persimmon tannin bioadsorbent	MO	225.70	[4]
PPy nanofibers	MO	173.01	[9]
Ferroferric oxide/polypyrrole magnetic	MO	149.48	[11]
Spent tea leaves (STL) modified with PEI	MO	62.11	[14]
MChs/Ppy	MO	89.28	[16]
Polypyrrole/SBA-15	MO	41.66	[17]
Fe_3O_4@SiO_2/PEI	MO	1058.4	[19]
MWCNTS@Fe_3O_4/PEI	MO	1727.60	[26]
ACF/GO/PEI	MO	237.50	[27]
Polypyrrole/CNTs-CoFe2O4	MO	116.69	[28]
PPy-PEI composite	**MO**	**232.56**	**Present work**

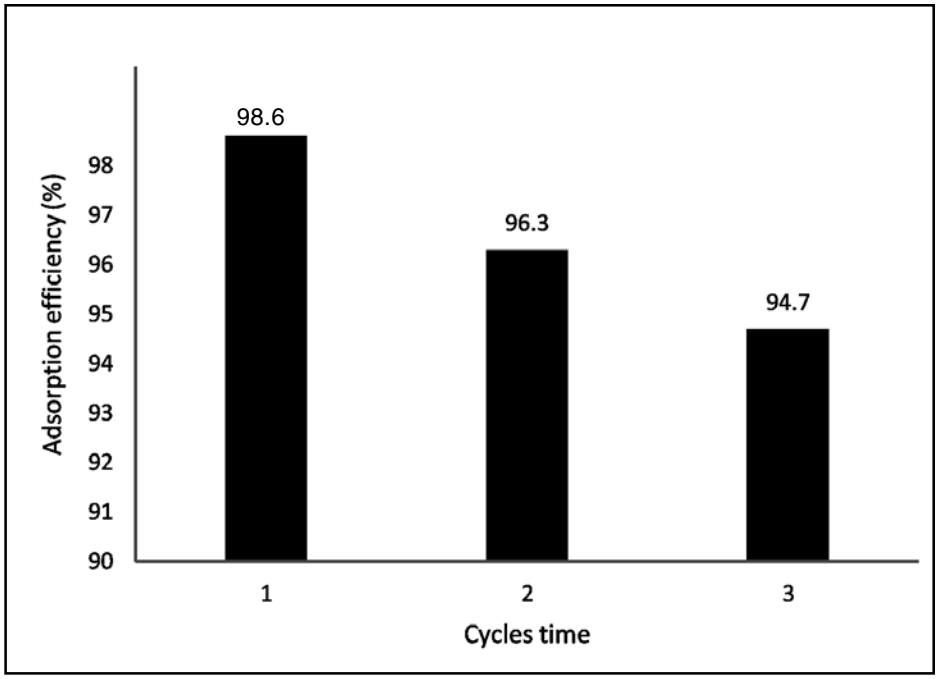

Fig. 13. Reusability of PPy-PEI adsorbent for MO adsorption.

regeneration study. It was crucial for an adsorbent's industrial applications for a facile regeneration [29]. The regeneration experiment was carried out with 50 mL of 0.1 M HCl or 50 mL of 0.1 M NaOH solution separately. From Figure 13, it demonstrates that MO dye adsorption and repeatability cycles were successfully carried out three times. MO dye adsorption efficiency decreased from 98.6 % to 94.7 % after three cycles. This decrease resulted from an increase in the dye ions that were strongly chemically bonded to the adsorbent following each cycle. The adsorbed PPy-PEI composite powder was subjected to several attempts of regeneration of the MO dye using 0.1 M HCl and 50 mL of 0.1 M NaOH solution, respectively. It was shown that the desorption of MO would be activated in a basic solution, of 0.1 M NaOH for the regeneration. Based on the results, it can be concluded that the PPy-PEI composite is appropriate for recycling and repeatedly serving as an effective adsorbent for MO dye removal because the removal efficiency is still high after three cycles. Similar findings have been reported by other authors [9,29,30-33].

CONCLUSION

In this present study, pristine polypyrrole (PPy) and polypyrrole-polyethyleneimine (PPy-PEI) polymer composites as conducting polymer-based adsorbents were successfully synthesized via chemical oxidative polymerization. The produced PPy-based adsorbents were characterized by BET, FESEM, ATR-FTIR, and XRD analysis for the formation of PPy-PEI polymer composite and its application as methyl orange (MO) dye adsorbent. It has been found that the maximum dye adsorption efficiency shown by both pristine PPy and PPy-PEI adsorbent were prepared from using 1:1 mole ratio of monomer to oxidant. It was found that the BET surface area of PPy-PEI composite was significantly higher with more binding sites as an adsorbent due to the availability of more amine groups than pristine PPy and therefore turned out to be far better an adsorbent than pristine polypyrrole. The Langmuir isotherm model appeared as a good fit for MO dye adsorption while the kinetic study followed the pseudo-second-order kinetic model. The regeneration study shows that the desorption of MO is preferred in basic solution and the adsorption efficiency remained high after three adsorption-desorption cycles.

References

1. S. A. Alqarni. (2022). The performance of different silver-titanium dioxide core-shell loading into Poly(3-nitrothiophen) for efficient adsorption of hazardous brilliant green and crystal violet dyes, *International Journal of Polymer Science,* p. 275-287.
2. Y. D. Susanti, N. Afifah and R. Saleh. (2021). Preparation of LaMnO3/TiO2/NGP composites for methylene blue dye removal via adsorption and photosonocatalysis, *Journal of Physics,* 012003.
3. J. E. T. Nolasco, E. N. O. Caneba, K. M. V. Edquila, J. I. C. Espita and J. V. D. Perez. (2019). Kinetics and isotherm studies of methyl orange adsorption using polyethyleneimine-graphene oxide polymer nanocomposite beads, *Key Engineering Materials,* 801, p. 304-310.
4. X. Li, Z. Wang, J. Ning, M. Gao, W. Jiang, Z. Zhou and G. Li. (2022). Preparation and characterization of a novel polyethyleneimine cation-modified persimmon tannin bioadsorbent for anionic dye adsorption, *Journal of Environmental Management,* 217, p. 305-314.
5. F. Mohamed, M. R. Abukhadra and M. Shaban. (2018). Removal of safranin dye from water

using polypyrrole nano-fiber/Zn-Fe layered double hydroxide nanocomposite (Ppy NF/Zn-Fe LDH) of enhanced adsorption and photocatalytic properties. *Science of The Total Environmental,* 640-641, p. 352-363.

6. M. Hao, M. Qiu, H. Yang, B. Hu, X. Wang. (2021). Recent advances on preparation and environmental applications of MOF-derived carbons in catalysis, *Science of the Total Environment,* 760, 143333.

7. L. Bai, Z. Li, Y. Zhang, T. Wang, R. Lu, W. Zhou and S. Zang. (2015). Synthesis of water-dispersible graphene-modified magnetic polypyrrole nanocomposite and its ability to efficiently adsorb methylene blue from aqueous solution, *Chemical Engineering Journal,* 279, p. 757-766.

8. Y. Huang, J. Li, X. Chen and X. Wang. (2014). Applications of conjugated polymer-based composites in wastewater purification, *RSC Advances,* 4(107), p. 62160-62178.

9. Q. Xin, J. Fu, Z. Chen, S. Liu, Y. Yan, J. Zhang and Q. Xu. (2015). Polypyrrole nano-fibers as a high-efficient adsorbent for the removal of methyl orange from aqueous solution, *Journal of Environmental Chemical Engineering,* 3(3), p. 1637-1647.

10. A. A. Alghamdi, A. Al-Odayni, W. S. Saeed, M. S. Almutairi, F. A. Alharthi, T. Aouak and A. Al-Kahtani. (2019). Adsorption of azo dye methyl orange from aqueous solutions using alkali-activated polypyrrole-based graphene oxide, *Molecules,* 3685.

11. M. Zhang, Z. Yu and H. Yu, Adsorption of Eosin Y. (2019). methyl orange and brilliant green from aqueous solution using ferroferric oxide/ polypyrrole magnetic composite, *Polymer Bulletin,* 7134.

12. M. Bhaumik, R. McCrindle and A. Maity. (2013). Efficient removal of Congo red from aqueous solutions by adsorption onto interconnected polypyrrole–polyaniline nanofibres, *Chemical Engineering Journal,* 228, p. 506-515.

13. N. S. Alsaiari, A. Amari, K. M. Katubi, F. M. Alzahrani, F. B. Rebah and M. A. Tahoon. (2021). Innovative magnetite based polymeric nanocomposite for simultaneous removal of methyl orange and hexavalent chromium from water, *Processes,* 9:576.

14. S. Wong, Tumari, H. Hasnaa, N. Ngadi, N. B. Mohamed, O. Hassan, R. Mat, A. Saidina, Aishah. (2018). Adsorption of anionic dyes on spent tea leaves modified with polyethyleneimine (PEI-STL), *Journal of Cleaner Production,* p. 394-406.

15. J. Deng, X. Wang, J. Guo and P. Liu. (2014). Effect of the oxidant/monomer ratio and the washing post- treatment on electrochemical properties of conductive polymers, *Industrial and Engineering Chemistry Research,* 53, p. 1380-13689.

16. F. Mashkoor and A. Nasar. (2020). Facile synthesis of polypyrrole decorated chitosan-based magsorbent: Characterizations, performance, and applications in removing cationic and anionic dyes from aqueous medium, *International Journal of Biological Macromolecules,* p. 2761-2789.

17. B. Boukoussa, A. Hakiki, S. Moulai. (2018). Adsorption behaviors of cationic and anionic dyes from aqueous solution on nanocomposite polypyrrole/SBA-15, *Journal Material Science,* 53, p. 7372–7386.

18. M. Varga, J. Kopecka, Z. Moravkova, I. Knvka, M. Trchova, J. Stejskal and J. Prokes. (2015). Effect of oxidant on electronic transport in polypyrrole nanotubes synthesized in the presence of methyl orange, *Journal of Polymer Science, Part B: Polymer Physics,* p. 1147-1159.

19. B. Huang, Y. Liu, B. Li, H. Wang and G. Zeng. (2019). Adsorption mechanism of polyethyleneimine modified magnetic core-shell Fe_3SO_4@SiO_2 nanoparticles for anionic dye removal, *RSC Advances,* 9, p. 32462-32471.

20. T. W. Seow and C. K. Lim. (2016). Removal of dye by adsorption: A review, *International Journal of Applied Engineering Research,* 11(4), p. 2675-2679.

21. R. S. Aliabadi and Mahmoodi, N. O. (2018). Synthesis and characterization of polypyrrole, polyaniline nanoparticles and their nanocomposite for removal of azo dyes; sunset yellow and Congo red, *Journal of Cleaner Production,* 179, p. 235-245.

22. M. Sulyman, J. Kucinska-Lipka, M. Sienkiewicz and A. Gierak. (2021). Development, characterization and evaluation of composite adsorbent for the adsorption of crystal violet from aqueous solution: Isotherm, kinetics, and thermodynamic studies, *Arabian Journal of Chemistry,* 103115.

23. S. Agarwal, I. Tyagi, V. K.Gupta, F. Golbaz, A. N. Golikand and O. Moradi. (2016). Synthesis and characteristics of polyaniline/zirconium oxide conductive nanocomposite for dye adsorption application, *Journal of Molecular Liquids,* 218, p. 494-498.

24. H. N. Bhatti, Y. Safa, S. M. Yakout, O. H. Shair, M. Iqbal and A. Nazir. (2020). Efficient removal of dyes using carboxymethyl cellulose/alginate/ polyvinyl alcohol/rice husk composite: Adsorption/desorption, kinetics and recycling studies, *International Journal of Biological Macromolecules,* 150, p. 861-870.

25. X. Quan, Z. Sun, H. Meng, Y. Han, J. Wu, J. Xu, Y. Xu and X. Zhang. (2018). Polyethyleneimine (PEI) incorporated Cu-BTC composites: extended applications in ultra-high efficient removal of congo red, *Journal of Solid State Chemistry,* p. 11223-11250.

26. B. Chen, W. Yue, H. Zhao, F. Long, Y. Cao and X. Pan. (2019). Simultaneous capture of methyl orange and chromium(VI) from complex wastewater using polyethyleneimine cation decorated magnetic carbon nanotubes as a recyclable adsorbent, *RSC Advances,* 9:4722.

27. L. Wang, M. Zhang, Q. Huang, C. Zhao, K. Luo and M. Lei. (2018). Fabrication of ACF/GO/PEI composite for adsorption of methyl orange from aqueous solution, *Journal of nanoscience and nanotechnology,* p. 1747-1756.

28. X. Li, H. Lu, Y. Zhang and F. He. (2017). Efficient removal of organic pollutants from aqueous media using newly synthesized polypyrrole/CNTs-CoFe2O4 magnetic nanocomposites, *Chemical Engineering Journal,* 316, p. 893-902.

29. A. Salama. (2017). Preparation of CMC-g-P(SPMA) super adsorbent hydrogels, Exploring their capacity for MB removal from waste water. *International Journal of Biological Macromolecules,* 106, p. 940-946.

30. X. Zhong, Z. Lu, W. Liang and B. Hu. (2020). The magnetic covalent organic framework as a platform for high performance extraction of Cr (VI) and bisphenol a from aqueous solution, *Journal of Hazardous Materials,* 393, 122353.

31. M. Maqbool, H. N. Bhatti, S. Sadaf, M. Zahid and M. Shahid. (2019). A robust approach towards green synthesis of polyaniline-Scenedesmus biocomposite for wastewater treatment applications, *Materials Research Express,* 6(5), 055308.

32. S. Noreen, H. N. Bhatti, M. Iqbal, F. Hussain and F. M. Sarim. (2020). Chitosan, starch, polyaniline and polypyrrole biocomposite with sugarcane bagasse for the efficient removal of Acid Black dye, *International Journal of Biological Macromolecules,* 147, p. 439-452.

33. P. Saharan, A. K. Sharma, V. Kumar and I. Kaushal. (2019). Multifunctional CNT supported metal doped MnO_2 composite for adsorptive removal of anionic dye and thiourea sensing, *Material Chemistry and Physics,* p. 239-249.

Received: 03-08-2023

Accepted: 15-10-2023